JOURNAL OF MATERIALS SCIENCE 29 (1994) 4157–4166

The influence of powder packing on the rheology of fibre-loaded pastes

S. BLACKBURN*, H. BÖHM
*IRC in Materials for High Performance Applications, * and also the School of Chemical Engineering, The University of Birmingham, Edgbaston, Birmingham, B15 2TT, UK*

The effects of fibre addition on the extrusion rheology of ceramic particulate pastes has been investigated using model pastes containing chopped glass fibre and alumina powders. In these pastes where the fibre diameter was much larger than the alumina particle diameter, there was a decrease in the pressure required to extrude the paste as the powder component was replaced by fibre, up to a ratio of 0.4 powder to 0.6 fibre by volume. When the pastes were characterized using physically based models this behaviour was reflected in lower values of the derived rheological parameters. It is shown that this behaviour can largely be attributed to the packing behaviour of the fibre and powder-phase components. The results also suggest that the presence of fibres increases the die entry pressure drop relative to the die land pressure drop. It is shown that while the models proposed by Milewski in combination with the rheological models can be used to illustrate the expected behaviour of composite pastes, the observed behaviour was better predicted by using modified models proposed by Karlsson and Spring. At high fibre loadings (> 60 vol %), extrudable materials could not be formed; this was attributed to packing and mixing problems leading to increased fibre–fibre interaction preventing flow. This is highlighted by materials in which the ratio of powder to fibre was 1 to 4 by volume, where the paste-like body was compressible and exhibited some elastic spring-back. For pastes where the solid phase contains < 50 vol % fibre the rheological behaviour is predictable if the packing behaviour of the fibre and the rheological behaviour of the pastes containing only the powder are known. This can be used as a tool to aid the design of composite pastes and for the development of suitable process equipment.

1. Introduction

There has been an increasing call for high-density ceramics and many processes have been investigated for the production of high green density components. One potential route is paste extrusion, where it has been shown that high-quality compacts can be produced [1]. Such pastes can be considered as two-component systems containing a continuous liquid or binder phase and a discontinuous, dispersed solid or particulate phase. When the two phases are mixed in the correct proportions the resultant paste will flow under an applied pressure yet retain its shape once the pressure is removed. The liquid phase is present in sufficient volume to fill the pores between the solid phase and to provide a small amount of excess liquid to overcome interparticulate friction by lubrication. As a result, the extrusion takes place close to the critical point in the drying curve and this aids in minimizing the internal stresses resulting in high green density compacts. The density of the packed powder bed can be increased by mixing powders of different sizes [2, 3] and in extrusion this can reduce the usage of liquid and yield bodies of greater density [4].

The need for improved mechanical performance has led to increased use of composite technology including the addition of fibres which can be continuous or short-chopped fibre filaments. Conceptually, such fibres can be added to a ceramic paste and extruded.

The addition of particles of high aspect ratio to low-viscosity liquids results in a thickening of the suspension over and above that brought about by the addition of a similar volume of spherical particles [5]. The greater the aspect ratio the greater the increase in apparent viscosity due to fibre–fibre interaction. The dispersion of fibres is thus restricted to relatively short-chopped materials, if balling and clumping is to be prevented. This might suggest that as fibres are added to pastes a stiffening of the system will occur. The rheological behaviour of fibre-loaded particulate pastes which are deformable at room temperature has not been systematically studied, though it has been shown that where the fibre diameter is much greater than the powder diameter, the pressure required for extrusion can be reduced [6]. Further, it has been shown that pastes resulting in dried extrudates containing 20 vol % fibre of an aspect ratio of 5 can be formed having green densities in excess of 60% theoretical density of the sintered body. A critical aspect in the further development of composite materials by plastic forming routes such as extrusion and injection

0022–2461

moulding is the relationship between fibre loading and the resultant rheology, so that design procedures for both paste and equipment can be developed.

In this paper the effects of fibre additions on the rheological behaviour of pastes and the relationships between the observations and the packing characteristics of the system are investigated. Model pastes based on glass fibre and alumina mixtures are considered. Their rheological behaviour is characterized using physically based equations, developed specifically for modelling paste extrusion by Benbow *et al.* [7]. This approach has been adopted because it yields information on the die entry as well as the parallel flow region of the extrusion system, and is thus preferred for these studies over standard capillary rheometry which yields apparent viscosity.

2. Experimental procedure

2.1. Solids composition

Two alumina powders were selected to be combined with glass fibre, a fused alumina (WFA F1500, Universal Abrasives Ltd, UK), which showed high sphericity but low roundness and high grain density with a median particle size, d_{50}, of 2.9 μm, and a calcined alumina (RA 107 LS, Baco, BA Chemicals, UK), which showed tabular habit with a d_{50} of 0.5 μm. The particle size distributions of the two powders, determined by X-ray sedimentation (Sedigraph, Micromeritics, UK, (manufacturers data)), are shown in Fig. 1. The glass fibre (Corning Glass, UK) had a mean diameter of 15 μm and mean length of 40 μm. The length distribution of the fibres was determined by measuring approximately 1000 individual fibres dispersed on a glass slide, the derived curve of fibre length is given in Fig. 2.

Two methods were used to determine the packing properties of the powders and the fibre: tap density and water absorption test (WAT). The tap density was determined by placing a total of 50 g material in a measuring cylinder and repeatedly dropping it (20 times) from a height of 40 mm on to a hard rubber mat. The volume of the tapped material was read directly from the cylinder and the density calculated.

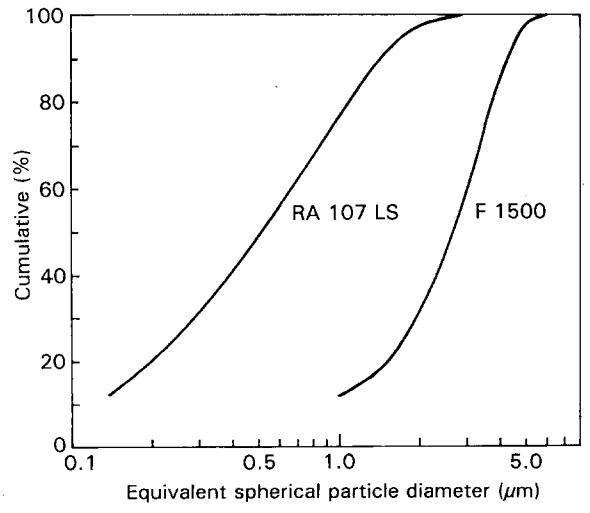

Figure 1 Powder particle-size distribution.

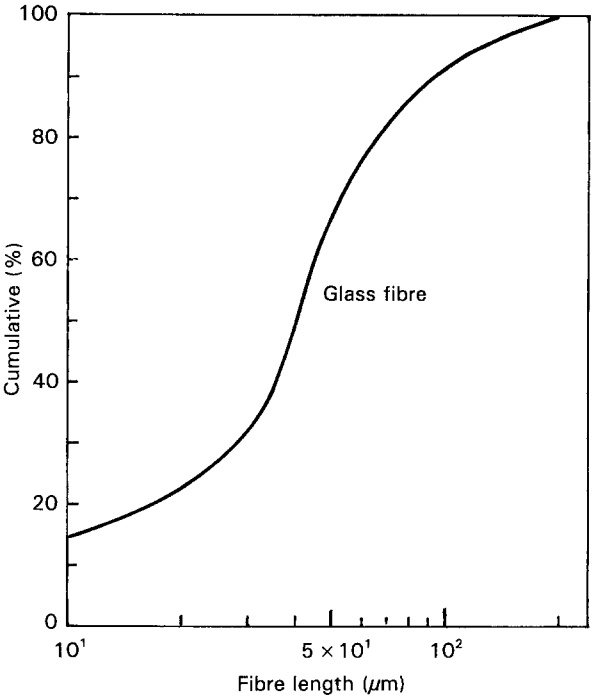

Figure 2 Fibre-length distribution.

For the determination of water adsorption, 2 g material were weighed on to a glass plate. Water was added dropwise from a burette and the mixture kneaded with a spatula. The end point was taken when a coherent paste was just formed. The ratio of mass of water to mass of material at this point were converted to relative packing density, ρ_p, using

$$\rho_p = \frac{(M_s/\rho_s)}{(M_s/\rho_s) + (M_l/\rho_l)} \quad (1)$$

where M_s and M_l are the mass of the solid and liquid phases, respectively, and ρ_s and ρ_l are the densities of the solid and liquid phases, respectively.

Errors can occur with both methods. With the tap density method, the interparticulate forces may prevent maximum packing. In the WAT test the results depend on the ability to mix the two components and to determine accurately the end point.

2.2. Liquid-phase composition (binder)

An 8 wt % solution of hydroxypropylmethylcellulose (HPMC) (Celacol B2/15, Courtaulds Chemicals, UK) in deionized water was maintained for all of the experimental work.

2.3. Paste preparation

The dry ingredients of alumina, glass fibre and HPMC powder were weighed and mixed dry in a planetary mixer for 10 min and then transferred to a Werner and Pfleiderer kneading machine. The appropriate amount of deionized water was added to yield the desired binder concentration. The mix was kneaded for 30 min, stopping occasionally to return manually any materials sticking to the walls of the mixer to the main body of material. The jacketted kneading ma-

TABLE I Paste composition and rheological character

Powder	Paste composition (vol %)			Paste parameters			
	Powder	Fibre	Liquid volume	σ_0 (MPa)	α (MPa s m^{-1})	τ_0 MPa	β (MPa s m^{-1})
RA 107LS	100	0	0.453	1.39	13.70	0.063	2.82
$d_{50} = 0.5$ μm	100	0	0.459	1.08	10.33	0.048	1.95
	100	0	0.478	0.42	4.31	0.023	1.70
	100	0	0.492	0.27	2.43	0.019	1.22
	90	10	0.417	2.60	27.85	0.182	1.59
	90	10	0.432	1.77	21.79	0.107	1.62
	90	10	0.440	0.80	8.27	0.032	1.64
	90	10	0.447	0.58	5.97	0.026	1.49
	90	10	0.460	0.28	2.52	0.021	1.29
	90	10	0.474	0.14	1.21	0.022	0.96
	80	20	0.394	2.26	17.3	0.121	2.65
	80	20	0.412	0.89	7.19	0.037	2.09
	80	20	0.431	0.33	2.61	0.033	1.44
	80	20	0.449	0.21	1.03	0.026	0.77
	80	20	0.459	0.11	1.21	0.022	0.53
	80	20	0.465	0.08	1.30	0.027	0.33
	70	30	0.378	1.04	8.45	0.082	1.62
	70	30	0.393	0.65	4.67	0.028	1.65
	70	30	0.398	0.43	2.79	0.023	1.47
	70	30	0.405	0.32	3.10	0.031	1.45
	70	30	0.407	0.36	2.70	0.023	1.35
	70	30	0.421	0.12	1.62	0.028	0.72
	70	30	0.430	0.09	0.99	0.021	0.58
	70	30	0.437	0.10	0.63	0.017	0.48
	60	40	0.348	1.88	7.41	0.070	0.73
	60	40	0.358	0.74	2.92	0.031	1.72
	60	40	0.377	0.21	1.75	0.030	1.12
	60	40	0.392	0.26	1.35	0.020	0.52
	60	40	0.394	0.27	1.57	0.030	0.59
	40	60	0.319	1.13	0.00	0.036	1.31
	40	60	0.329	1.11	2.96	0.039	0.81
F1500	100	0	0.483	1.06	5.30	0.109	0.73
$d_{50} = 2.9$ μm	100	0	0.489	0.57	0.00	0.062	1.07
	100	0	0.492	0.67	0.00	0.046	1.00
	100	0	0.494	0.64	0.78	0.066	0.57
	100	0	0.504	0.49	0.14	0.053	0.80
	100	0	0.524	0.27	0.00	0.020	0.34
	80	20	0.432	1.56	16.44	0.073	1.23
	80	20	0.449	0.63	8.18	0.030	1.22
	80	20	0.465	0.26	4.27	0.021	0.83
	80	20	0.475	0.16	2.70	0.021	0.78

chine was cooled with flowing water to ensure that the mix maintained a constant temperature of 18 °C.

Pastes were formulated to give different volumetric fibre contents in the solid phase of 0, 10, 20, 30, 40, 60 and 80 vol % for the calcined alumina ($d_{50} = 0.5$ μm) and 0 and 20 vol % for the fused alumina ($d_{50} = 2.9$ μm) relative to the total solids content. For each powder–fibre mix the liquid content was varied to give pastes of different consistency. The pastes were allowed to stand for 1 h before evaluating their rheological properties, to prevent any time-dependent behaviour of the paste system influencing the results. Thus, a total of 41 pastes were individually prepared and characterized. The compositions and rheological data for each paste is given in Table I.

2.4. Paste characterization

The flow behaviour of the pastes was characterized using physically based equations developed by Benbow *et al.* [7] in which up to six geometry-independent paste parameters can be derived. The model has been developed specifically for the analysis of extrusion and looks at both the convergent and the parallel flow of the paste. This method has been adopted here in preference to capillary analysis which yields apparent viscosities which are, in most cases, shear-rate dependent.

The equation relating the pressure drop, P, through a die of circular cross-section, of diameter D and length L from a barrel, also of circular cross-section, diameter D_0, where v is the extrudate velocity, is

given by

$$P = (\sigma_0 + \alpha_1 v^m)2\ln\left(\frac{D_0}{D}\right) + 4\left(\frac{L}{D}\right)(\tau_0 + \beta_1 v^n), \quad (2)$$

The paste parameters are σ_0, τ_0, α_1, β_1, m and n. The term $(\sigma_0 + \alpha_1 v^m)$ equates to the yield stress, σ, observed during the bulk deformation of the paste, σ_0 is the yield stress extrapolated to zero velocity. The factor α_1 and the exponent m characterize the effect of velocity on the yield stress. In the model it is assumed that pastes exhibit plug flow in capillaries (evidence for plug flow is common in the paste literature [7–9]) and that all shear takes place in a thin liquid layer at the die wall–paste interface. This enables a force balance to be derived which yields a wall shear stress at zero velocity, termed the initial wall shear stress, τ_0, and a factor, β_1, and an exponent n which account for the velocity dependence of the wall shear stress, τ. Therefore, σ_0 and τ_0 represent the quasi-static situation while α_1, β_1, m and n represent the dynamic situation. Where the relationship between pressure, P, and velocity, v, is essentially linear, a simplified model in which the velocity exponents are set at unity can be used

$$P = (\sigma_0 + \alpha v)2\ln\left(\frac{D_0}{D}\right) + 4\left(\frac{L}{D}\right)(\tau_0 + \beta v) \quad (3)$$

where α and β have different units to α_1 and β_1. Initial tests showed that this simplified relationship can be used to model the pastes reported in Table I and further, given the test procedure, it is known that the simplified model gives more reliable and internally consistent results. A typical fit is shown in Fig. 3.

The extrusion parameters, Table I, were evaluated using a ram extruder with a barrel diameter of 25.4 mm fitted with interchangeable dies of diameter 3 mm and lengths 3, 24 and 58 mm. The die entry semi-angle of all the dies was 90°, i.e. without conical taper. The ram was driven using a compressional load frame (Avery Denison, UK), from which load versus displacement curves were determined. For each die, approximately 150 g paste was extruded. By setting the crosshead speed, extrudate velocities ranging from 0.001–0.053 m s^{-1} were examined. From the data generated, the paste parameters were calculated. Details of the computational procedures are given elsewhere [7, 9, 10].

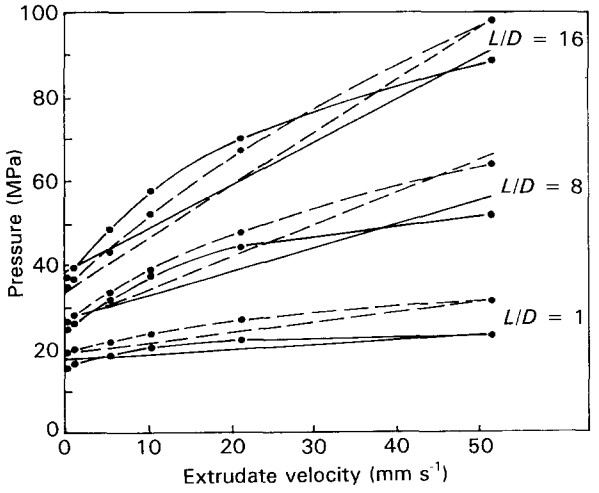

Figure 3 Pressure–velocity plots for two pastes showing (—●—, – –●– –) the experimental data and (—, – – –) the four-paste parameter fit quoted in Table I, for (– – –) 0% fibre, 47.8 vol % water, and (—) 20% fibre, 43.1 vol % water.

Three samples of approximately 10 g each of the extrudates were tested for moisture content, by drying for 18 h at 110 °C. This total moisture content represents the moisture present in all the constituents, including the very low moisture content (approximately 0.2 wt %) in the powders. The measured moisture contents were converted to volume percentages using

$$\text{volume per cent liquid} = \frac{(\lambda\xi/\rho_l)100}{(\lambda\xi/\rho_l) + ((100 - \lambda\xi)/\rho_s)} \quad (4)$$

where λ is the moisture content (wt %) and ξ is the ratio of the total mass of binder to moisture content (corrected for any solids content).

3. Results and discussion

3.1. Packing densities in the end-member powders

The results of the packing density tests are summarized in Table II. The TAP densities of the alumina powders were particularly low due to the powder being agglomerated. However, these agglomerates are generally weak and in the WAT test appear to have broken down to give the apparent increase in density. Thus, the WAT test result was favoured for these materials. The chopped fibre gave high-density values in the WAT test because when moist the fibres form self-supporting structures. Consequently, the tap density test was preferred for these materials. The mean aspect ratio of the fibres was approximately 3 and Milewski [10] shows that the packing density of stiff monosized fibres of similar mean aspect ratio would be approximately 64% compared to 70% for a mean aspect ratio of 1. The TAP density recorded for the fibres was 52%, significantly lower than 64%. This was attributed to there being a proportion of much longer fibres giving behaviour similar to the packing of monosized fibres with aspect ratio 7.

TABLE II Packing behaviour

Powder	Relative packing density by WAT	Relative packing density by TAP
Fine alumina (d_{50} = 0.5 μm)	0.56	0.31
Coarse alumina (d_{50} = 2.9 μm)	0.51	0.32
Glass fibre (mean length = 40 μm)	0.84	0.52

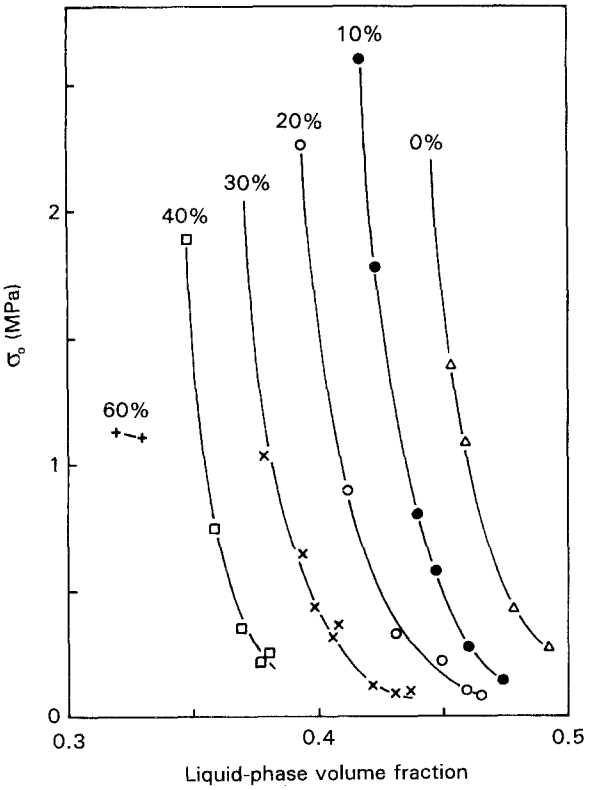

Figure 4 Yield stress, σ_0, liquid phase volume fraction curves for additions of fibre to fine calcined alumina (d_{50} = 0.5 μm). Per cent volume additions as given.

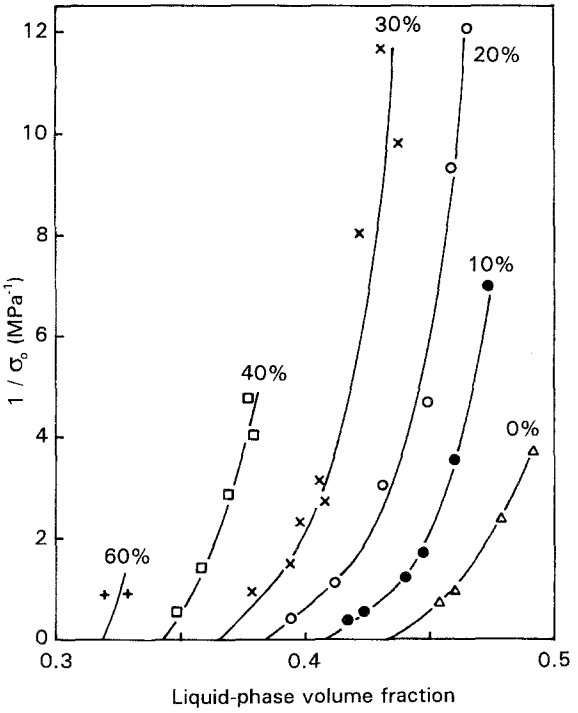

Figure 5 Reciprocal yield stress, $1/\sigma_0$, liquid phase volume fraction curves for various fibre loadings.

3.2. Fibre degradation during mixing

During the formation of pastes it is possible for some fibre breakdown to occur. When the pastes were dispersed in water and mounted on glass slides and the fibre lengths measured as before, the fibre length appeared to increase. This was attributed to difficulties in distinguishing the shortest fibres in the system from the matrix. In the findings of other workers the reduction in fibre length during mixing has often been small where the aspect ratio was low [4, 11, 12]. Therefore, significant change in fibre length distribution was not suspected.

3.3. The effect of moisture content and fibre loading on the wall shear stress, σ_0

The effect of moisture content and the fibre loading on the wall shear stress, σ_0, is shown in Fig. 4 for the pastes formed with the finer alumina. It can be seen that for any particular ratio of fibre to powder, σ_0 decreases as the moisture increases and that as moisture is reduced, σ_0 increases eventually to infinity, i.e. the paste was no longer extrudable. Given that the fluid is a suitable binder, extrusion only becomes possible when there is sufficient fluid present to separate and lubricate the particles. This allows them to pass over each other during convergent flow. The minimum amount of liquid required for extrusion appears to be when the liquid volume is equivalent to the pore volume of a packed bed of the solid phase. For example, in the paste containing no fibre and fine alumina, Table I, the volume of liquid at the point where σ_0 tends to infinity is 42% and, if there is no gas entrapment (pastes are well mixed and incompressible), the solid volume will be 58%; this value compares very closely with the WAT packing density reported in Table II. It is simpler to estimate the liquid volume where σ_0 becomes infinite by plotting the reciprocal of the parameter against the liquid volume and taking the value where $1/\sigma_0 = 0$, Fig. 5. Lubrication rapidly increases above this critical liquid concentration and thus the extrusion pressure drops rapidly. The range of liquid to solid contents for practical extrusion is limited. For example if the value of σ_0 exceeds 2.0 MPa then the extrudates show strong discolouration due to die wear as lubrication is removed. If σ_0 falls below 0.2 MPa then the extrudates cannot retain shape. In the pastes containing the finer alumina, the moisture range for practical extrusion was approximately 2 vol %. The moisture range over which the pastes based on the coarser alumina (d_{50} = 2.9 μm) were extrudable was similar, but there was a significant increase in the overall moisture required for extrusion. This is illustrated in Fig. 6. The increase in required moisture content is due to the narrower particle-size distribution of the fused and classified material which accordingly packed less well (in the WAT test). In pastes formed from both types of alumina there was a systematic fall in σ_0 with increasing fibre content at any given moisture content. Less moisture was required to give a constant σ_0 with increasing fibre loading. The drop in σ_0 between 0% and 20% fibre addition is similar in both alumina powder systems. In the pastes containing the finer tabular alumina, systematic drops in σ_0 were observed up to 40 vol % fibre addition, Fig. 4. In all these systems the internal structure of the extrudate was visually homogeneous. The 60 vol % fibre-loaded paste was extrudable, but there was a loss of textural

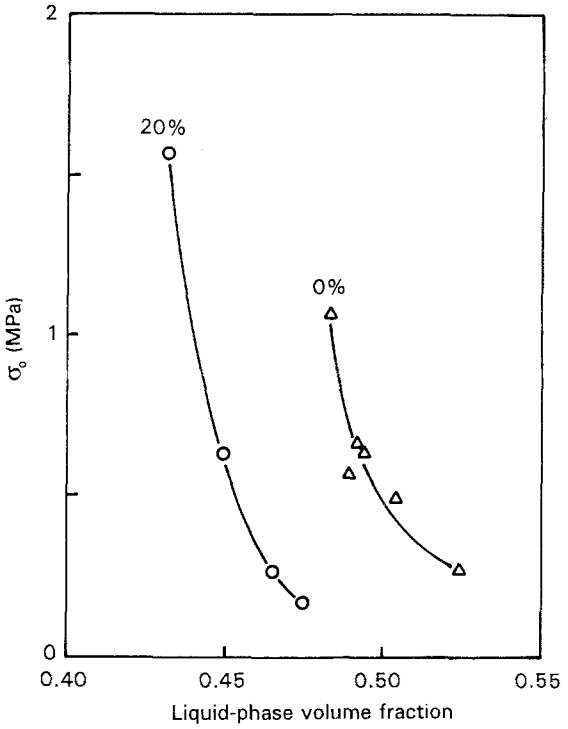

Figure 6 Yield stress, σ_0, liquid phase volume fraction curves for the addition of fibre to fused fine alumina (d_{50} = 2.9 μm). Per cent volume additions as given.

consistency and surface imperfections were common. However, σ_0 for these pastes showed similar trends to those observed in the 40 vol % fibre-loaded paste though the results were less consistent. Extrudable pastes could not be formed when the solid phase contained 80 vol % fibre. This material was deformable exhibiting spring-back when an applied load was removed. This spring-back can be attributed to two effects; the fibres can flex within their elastic limit as the load is applied because the fine powder is present in insufficient volume to fill the void space between the fibre network, and secondly because the paste contains insufficient fluid (determined by volume/weight loss calculation) to fill the pore volume leaving some compressible air within the body. The incomplete filling of the inter-fibre pores with liquid was confirmed by there being no observed moisture loss while the material was under load.

3.4. The effects of moisture control on all extrusion parameters

The accuracy of the determinative method leads to errors in the calculated parameters. The accuracy of σ_0 is approximately ± 10% while the accuracy of τ_0, α and β are reduced to approximately ± 20%, 30% and 40%, respectively [4]. Thus the accuracy of the dominant parameter is relatively high. The inaccuracies in the dynamic parameters are greatest in pastes where the influence of V is small, as in these materials. If the liquid phase were very viscous, α and β could be the dominant terms and σ_0 and τ_0 would then be less accurate. In addition, in the system employed here, the entry effects are large and the land effects small, thus α is more accurate than β. These particular formulations result in low β values which lie below the lower limits of accurate measurements. Given these constraints, the trends observed are reasonably constant in all the paste parameters, as shown in Figs 7–9.

The systematic reduction in paste parameters with increasing fibre loading can be explained by the addition of fibres changing the relative degree of lubrication. Contributions from fibre–fibre, fibre–particle and fibre–extruder wall interactions can also be expected. As packing is known to bring about major changes in paste rheology, the relationship between simple packing theory and the observed rheology is considered first.

3.5. Packing theory

3.5.1. Packing of spherical powders

Packing relationships can be diagramatically represented by plotting the mix composition against the relative bulk volume, where 1.0 is equal to 100% solids by density and 2.0 equals 50% solids by density or the reciprocal of volume fraction. Fig. 10 is constructed for the perfect packing for powders of perfect spheres of two different sizes, where $R = 0$ (R is the ratio of the diameter of the small particles to the diameter of the large particles) i.e. the fine fraction is infinitely smaller than the coarse fraction. This representation allows curves for $R = 0$ to be drawn as straight lines [13] such that,

$$V = Cx \tag{5}$$

for the region where small spheres are filling the interstitial voids between coarse particles and,

$$V = x + Fy = x + F(x - 1) \tag{6}$$

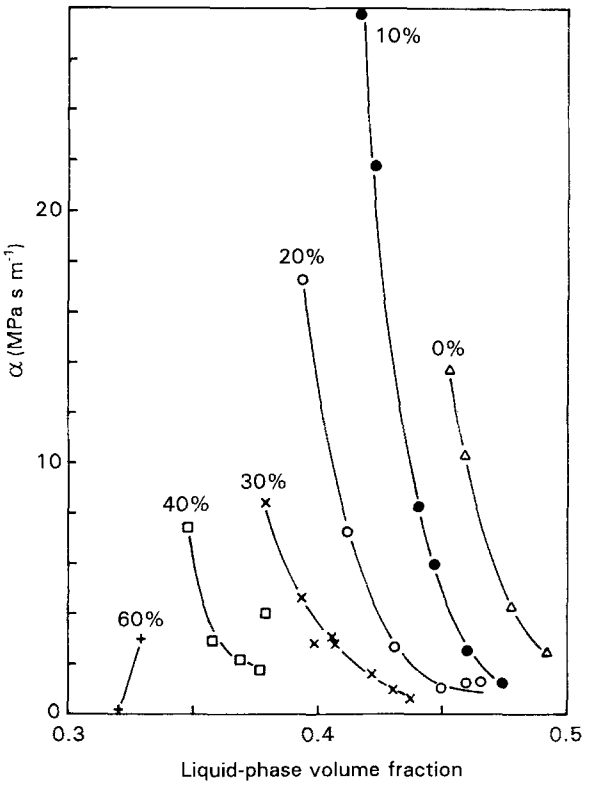

Figure 7 Die entry velocity factor, α, liquid phase volume fraction curves for additions of fibre to fine calcined alumina (d_{50} = 0.5 μm).

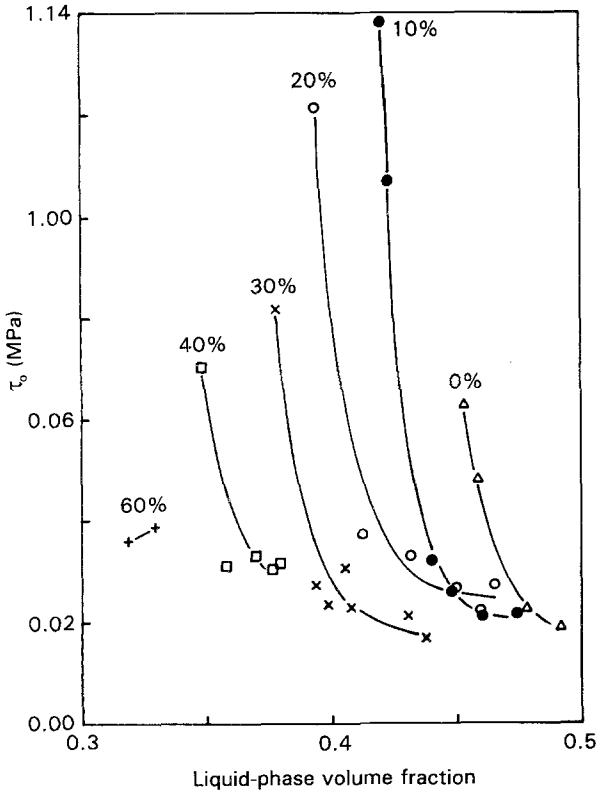

Figure 8 Die wall shear stress, τ_0, liquid phase volume fraction curves for additions of fibre to fine calcined alumina (d_{50} = 0.5 μm).

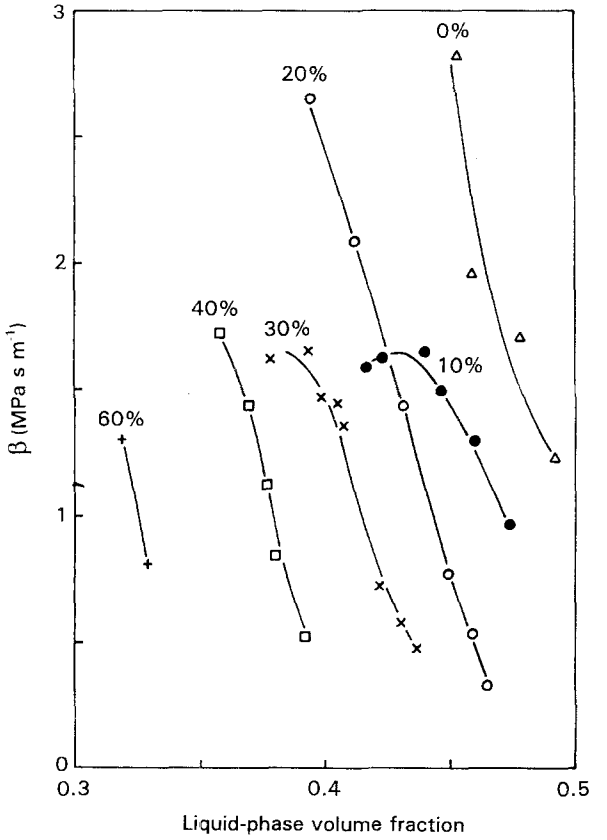

Figure 9 Die land velocity factor, β, liquid phase volume fraction curves for additions of fibre to fine calcined alumina (d_{50} = 0.5 μm).

for the region where large spheres are replacing many small spheres and their voids; where V is the relative bulk volume, x is the volume fraction of the coarse powder and y is the volume fraction of the fine powder, C, is the relative bulk volume of the coarse fraction, and F is the relative bulk volume of the fine fraction.

Taking the packing density of the fine alumina powder, F_p, and assuming that a coarse powder fraction would pack similarly, C_p, a second plot can be constructed for this more realistic situation, also shown in Fig. 10. It can be seen from this simple model that the maximum packing is reduced from point A to point B when the materials contain imperfect spheres and that the optimum mixture contains a greater proportion of fines. Karlsson and Spring [14] show that in non-ideal powders this shift is even greater, and they present a corrected model. Other workers [15] have demonstrated this shift experimentally.

3.5.2. Fibre systems

It is possible to substitute fibre into the simple model [13] to generate new curves. Two situations can be envisaged with fibres in which R becomes R', where R' is defined as the diameter of a sphere divided by the diameter of the fibre (note: fibre aspect ratio is not accounted for directly but is included in terms of the initial packing density). Thus, R' may therefore range from 0 to ∞ at the two extremes. When R' is 0, the fibres are infinitely greater in diameter than the powder and low R' values are often found in ceramic matrix composites (CMCs).

The packing density of fibres is normally much less than that of spheres. The packing behaviour if all the fibres align, is shown in Fig. 10, C_{FT}, for $R' = 0$. A maximum occurs at point K. Fig. 11 shows the relationship for the experimental packing data for the two

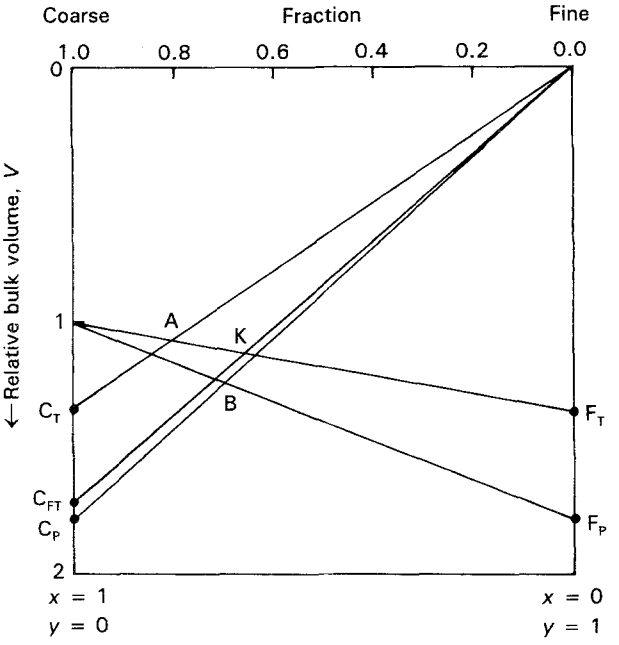

Figure 10 Relative bulk volume plots for mixtures of perfect spheres of two infinitely different sizes, line C_T (coarse theoretical packing), A, F_T (fine theoretical packing), mixtures of experimental powder (d_{50} = 0.5 μm) and similar packing infinitely coarser powder, line C_P (coarse powder packing), B, F_P (fine powder packing), and mixtures of perfectly spherical fine powder with infinitely larger fibre exhibiting maximum packing (line C_{FT} (coarse theoretical powder packing), K, F_T).

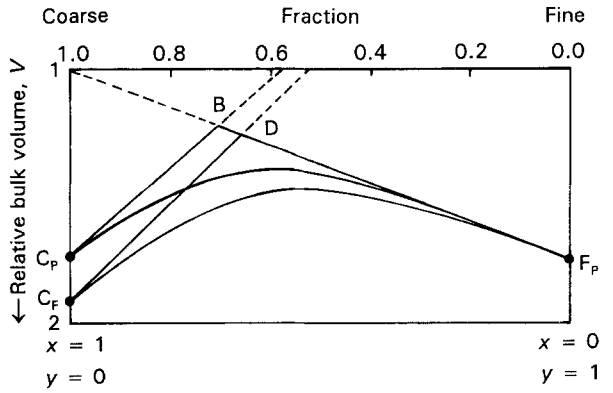

Figure 11 Relative bulk volume plots for mixtures of the experimental powder (d_{50} = 0.5 μm) and a theoretical infinitely coarser powder exhibiting similar packing behaviour (line C_P, B, F_P), and mixtures of experimental powder (d_{50} = 0.5 μm) and experimental fibre (line C_F, D, F_P) assuming infinite size difference, R and R' = 0. The curved lines represent mixtures where the two components are closer in size, R and R' = 0.125.

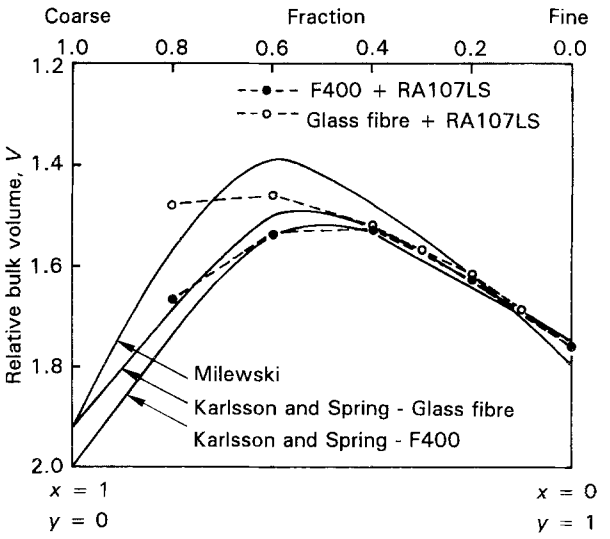

Figure 12 Relative bulk volume plots comparing experimental points derived from Fig. 5 and lines predicted using packing theory for R' = 0.03 and R' = 0.

end members used in this study, yielding a maximum at D, and contrasts them with near spherical data where the maximum occurs at B.

Two further lines are plotted in Fig. 11 for an intermediate value of R and R' of 0.125. These lines were derived using

$$\left(\frac{V - Cx}{F}\right) + 2G\left(\frac{V - Cx}{F}\right)\left(\frac{V - x - Fy}{C - 1}\right) + \left(\frac{V - x - Fy}{C - 1}\right)^2 = 1 \quad (7)$$

where G is a factor related to R or R' [16].

From these plots it can be deduced that the mixing of coarse fibres with fine powders will lead to higher packing densities and that at the maximum a greater proportion of fines will be present than when both powders are near spherical. Where $R' = 0$ and the mixture lies in the region where the large fibres are replacing the fine powder, the packing density will be the same as for a system where $R = 0$. The separation of the two maxima is governed by the packing density of fibres. Clearly as the fibres become shorter they tend to resemble spheres and hence pack more closely, moving C_f towards C_p and D towards B, in Fig. 11. If the fibre is only slightly larger in diameter than the powder, it can be seen that by the application of Equation 7, the maximum packing for the fibre–sphere system will be less than for the sphere–sphere system as before. However, in this case, small additions of fibre will yield lower packing densities than equivalent additions of large spheres to the same fine powder. The fibre–sphere system always packs less well than an equivalent sphere–sphere system.

3.5.3. Present study

All the intercepts in Fig. 5 were converted to relative bulk volume and plotted with the predicted curves of the Milewski approach for R' = 0.03 (R' for the experimental powders) on a relative bulk volume diagram, Fig. 12. It can be seen that the fibre-loaded materials closely follow the predicted behaviour up to 20 vol % addition. Above that fibre loading, the apparent packing density of the paste is reduced compared to the predicted line up to 60 vol %. The 80 vol % paste could not be extruded and the point plotted is estimated from the mixing additions and tends to relate more closely to the WAT test data for 100% fibre, Table II. Both the 100 and 80 vol % fibre values lie above the predicted line due to the interlocking behaviour of these highly fibrous materials. The experimental points derived from the paste data do not lie close to the line predicted by Milewski's approach. It has already been mentioned that with irregular particles there is a discrepancy between such simple models and practical observation in "real" systems. Based on the work of Karlsson and Spring, new predictions correcting for both intermediate R' values and irregular particles can be derived. These curves are shown in Fig. 12. It can be seen that the derived curves fit the experimental findings better where the coarse fraction is less than 60 vol %. The slight apparent increase in packing for the fibre-loaded pastes compared to the prediction of Karlsson and Spring in this region, may be due to fibre interactions, or possibly due to fibre size-reduction processes during mixing, effectively increasing the packing potential of the fibre.

Further experiments were carried out in which the fibre was replaced by a similar volume of coarse α-alumina powder, where the average volume of each grain was equal to the average volume of each fibre to evaluate the influence of fibre interactions. For this, a powder of mean diameter 22 μm was used (WFA F400, Universal Abrasives Ltd, UK) with a WAT relative packing density of 0.5. The replacement was carried out for 20, 40 and 60, and 80 vol % additions. The packing density could be calculated for the coarse particulate paste using the same routines and the results are shown in Fig. 12. A predictive curve for this paste derived by the application of the Karlsson and Spring approach is also given in Fig. 12. There was

little difference in the behaviour of the two types of paste up to 60 vol % additions of the coarse fraction, though the fibre-loaded pastes generally gave slightly higher packing. This shows that the fibre is having little additional effect on the paste behaviour. As the coarse loadings increased above 60 vol % the pastes showed different behaviour depending on the shape of the addition. The fibre-loaded pastes showed apparently high densities due to fibre–fibre interaction leading to self-supporting structures without complete filling of the pore space, while the pastes containing the coarse spherical grains follow the predicted line more closely.

It was found that similar relationships exist for the other paste parameters. This is to be expected, because the point being used to predict the packing behaviour is when extrusion becomes impossible, i.e. when all parameters become infinite. The packing relationships clearly control the onset of extrusion. As liquid is added, the extrusion requires less load and this results in lower parameters. This can be represented on a relative bulk volume plot where the reciprocal parameter contours are plotted, Fig. 13. There are however, some subtle differences in the behaviour of the pastes as they become softer by the addition of liquid, shown by the differences in contour spacing in Fig. 13.

The ratio of the yield stress to initial wall shear stress (σ_0/τ_0) varied with moisture content for any particular mix of powder and fibre. At high moisture contents the ratio averaged 7.5 and as the moisture content decreased, the ratio increased to an average of 22.3. Frequently, in the stiffest paste of any powder–fibre series, the σ_0/τ_0 ratio fell slightly from the highest value. There was slight increase in the ratio as more fibres were added (31.5 in 60 vol %). The observed ratios in these pastes were high compared to those observed in pastes bound with non-polymer systems [4]. In pastes made from spherical powders, this ratio is reduced in intermediate mixtures of coarse and fine materials, an opposite trend to that reported here. This is an indication that increased fibre interaction occurs in the die entry as the fibres are forced to rotate and move past each other to align in the die land.

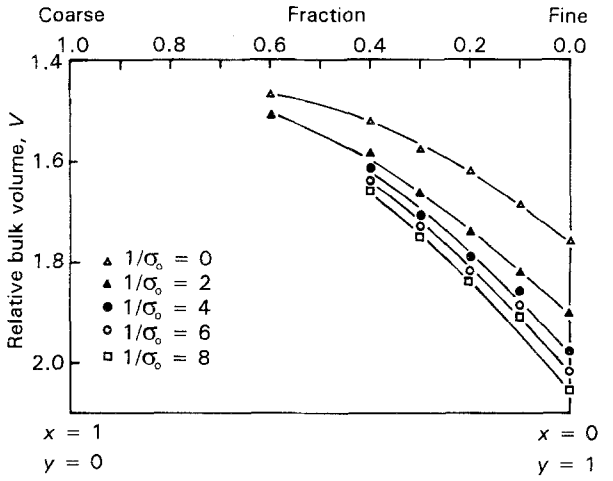

Figure 13 Relative bulk volume plot showing the apparent packing density of the solids for different values of reciprocal yield stress ($1/\sigma_0$).

The differences under flow are relatively small and thus, with particle packing being the major contributor to the paste behaviour in chopped-fibre systems, predictive estimates of paste behaviour can be made. If the packing behaviour of the fibre, the rheological behaviour of the particulate matrix, and the size ratio of the two fractions are known, then it should be possible to predict the behaviour of any intermediate composition. For this to be possible it must generally be assumed that rheological behaviour of the pastes with respect to moisture additions above the critical point are constant. Thus, referring to Fig. 13, to produce a paste containing 15 vol % fibre with a yield stress, σ_0, of 0.25 MPa, 45.2 vol % liquid phase would have to be added.

The data presented by Stedman *et al.* [17] suggest that the viscosity increases with 20% fibre additions in injection-moulding suspensions. This, at first sight, appears to contradict the observations reported here. However, the fibres used in their work had similar diameters to the powder and, as a consequence, the predicted packing behaviour would be represented by a near straight line between the two end-member densities, C and F, so

$$V = Cx + Fy \tag{8}$$

Under these conditions, a paste would require more force to be extruded than the purely fine particulate liquid system as the volume of liquid required to fill the pore space would be increased.

4. Conclusion

The rheology has been examined for a range of alumina pastes containing glass fibre as a coarse fraction addition. This has enabled the effects of fibre additions to ceramic paste systems to be studied and related to packing behaviour predictions using simple models. At low fibre loadings (< 50 vol %) it has been shown that where the fibres are of much larger diameter than the matrix particles, the pastes become easier to extrude at any given liquid content. The behaviour of the system at low fibre loadings can be attributed almost entirely to the packing behaviour of the powder and fibre, there being little, if any, effect due to the fibre interactions. At higher fibre loading (> 50 vol %), fibre–fibre interaction is such that there is no direct link to predictable packing behaviour. The location of the transition from predictable packing-dominated to interaction-dominated behaviour will vary depending on the nature and aspect ratio of the fibre. The models of Karlsson and Spring, which predict the packing of irregular particles in combination with the principles of Milewski on fibre packing, compare favourably with the packing densities derived from extrusion data. The results indicate the rheological behaviour of pastes containing short chopped fibres are predictable at low fibre additions by combining simple packing theory with physical paste rheology characterization. This offers a useful tool for composite paste development.

Acknowledgements

The authors are grateful to the SERC for their support.

References

1. M. J. HANNEY and R. MORREL, *Proc. Br. Ceram. Soc.* **32** (1982) 277.
2. C. C. FURNAS, *US Bur. Mines, Bull.* **307** (1929).
3. M. CROSS, W. H. DOUGLAS and R. P. FIELDS, *Powder Technol.* **43** (1985) 27.
4. S. BLACKBURN and H. BÖHM, *Chem. Eng. Res. Design, Trans. IChemE* **71** (A3) (1993) 250.
5. B. CLARKE, *Trans. Inst. Chem. Eng.* **45** (1967) 251.
6. S. BLACKBURN, in Proceedings of the Materials Research Society, Vol. 289 "Flow and Microstructure of Dense Supensions", edited by L. J. Struble, C. F. Zukoski and G. C. Maitland (MRS, Pittsburgh, PA, 1993) pp. 135–139.
7. J. J. BENBOW, E. W. OXLEY and J. BRIDGWATER, *Chem. Eng. Sci.* **42** (1987) 2152.
8. J. J. BENBOW, T. A. LAWSON, E. W. OXLEY and J. BRIDGWATER, *Am. Ceram. Soc. Bull.* **68** (1989) 1821.
9. J. J. BENBOW, *Chem. Eng. Sci.* **26** (1973) 1467.
10. J. V. MILEWSKI, *Adv. Ceram. Mater. Am. Ceram. Soc.* **1**(1) (1986) 36.
11. T. A. LAWSON and S. BLACKBURN, *J. Am. Ceram. Soc.* **75** (1992) 953.
12. J. STEDMAN, J. R. G. EVANS and J. WOODTHORPE, *J. Mater. Sci.* **25** (1990) 1025.
13. J. V. MILEWSKI, *Ceram. Eng. Sci. Proc. Am. Ceram. Soc.* **12** (1991) 1095.
14. K. KARLSSON and L. SPRING, *J. Met. Sci.* **5** (1970) 340.
15. S. YERAZUNIS, J. W. BARTLETT and A. H. NISSAN, *Nature* **195** (1962) 33.
16. A. R. E. WESTMAN, *J. Am. Ceram. Soc.* **19** (1936) 127.
17. J. STEDMAN, J. R. G. EVANS and J. WOODTHORPE, *J. Mater. Sci.* **25** (1990) 1833.

Received 7 January
and accepted 9 February 1994